

# Electron impact excitation and dissociation of halogen-containing molecules

Masashi Kitajima,  
Ryoji Suzuki,  
Hiroshi Tanaka,  
Lukáš Pichl,  
Hyuck Cho

**Abstract** A systematic analysis of the absolute differential cross sections (DCSs) for electron scattering by halogen-containing molecules  $\text{CF}_3\text{X}$  ( $\text{X} = \text{H}, \text{F}, \text{Cl}, \text{Br}, \text{I}$ ) has been performed with impact energy and scattering angle ranging from 1.5 to 100 eV and 15 to 130°, respectively. Three of the results of these experiments are described in the present report. Firstly, a clear difference is demonstrated in the elastic-scattering cross section angular distributions of polar and nonpolar molecules with the substitution of one of the F atoms in  $\text{CF}_4$  for a H, Cl, Br or I atom. Secondly, vibrational excitation spectra of the unresolved composite modes (mainly  $\text{CF}_3$  stretching) for  $\text{CF}_3\text{X}$  reveal a common broad structure in the region from 7 to 9 eV due to shape resonance. The third result presented is the observation of a low-lying electronic state of  $\text{CF}_3\text{Cl}$ ,  $\text{CF}_3\text{Br}$ , and  $\text{CF}_3\text{I}$ . This feature is enhanced at lower incident energies and larger scattering angles. Also discussed are some preliminary results on the formation of negative and neutral fragments from  $\text{SiF}_4$  and  $\text{CH}_4$  by electron impact.

**Key words** crossed beam experiment • dissociation • dissociative attachment • differential cross section • electron impact • halogenated hydrocarbons

## Introduction

The halogenated methane derivatives  $\text{CF}_3\text{X}$  ( $\text{X} = \text{H}, \text{F}, \text{Cl}, \text{Br}, \text{I}$ ) are important industrial materials with wide-ranging applications in fields such as refrigeration and semiconductor etching. However, it is now widely recognized that  $\text{CF}_3\text{Cl}$  and  $\text{CF}_3\text{Br}$  contribute, via photochemical mechanisms, to the depletion of the earth's ozone layer that protects us from the damaging effects of short wavelength solar radiation. Furthermore, the plasma etching molecules  $\text{CF}_3\text{H}$  and  $\text{CF}_4$  are strong greenhouse gases and, therefore must be replaced by alternative compounds with low global warming potentials. One possible replacement is  $\text{CF}_3\text{I}$  since, due to the weakness of the C-I bond, it should be possible to produce high yields of the etching radical  $\text{CF}_3$  by direct electron impact. Thus, there is a practical as well as fundamental interest in obtaining quantitative spectroscopic information on these halogenated methane derivatives. Part of the experimental program is to determine quantitatively the electron collision cross sections for halogen-containing fluorocarbons, such as the DCSs for elastic scattering and for vibrational and electronic excitation. Detailed knowledge of electron collisions with complex molecules, in particular processes such as dissociation and dissociative attachment below the ionization threshold, is essential to understand the chemical reactions that occur in industrial plasmas and in the atmosphere.

M. Kitajima, R. Suzuki, H. Tanaka✉  
Department of Physics,  
Sophia University,  
Tokyo 102-8554, Japan,  
Tel.: +81/ 3 3238 3472, Fax: +81/ 3 3238 3341,  
e-mail: h\_tanaka@sophia.ac.jp

L. Pichl  
Department of Computer Software,  
The University of Aizu,  
Aizu-Wakamatsu 965-8580, Japan

H. Cho  
Physics Department,  
Chungnam National University,  
Daejeon 305-704, Korea

Received: 14 November 2002, Accepted: 21 January 2003

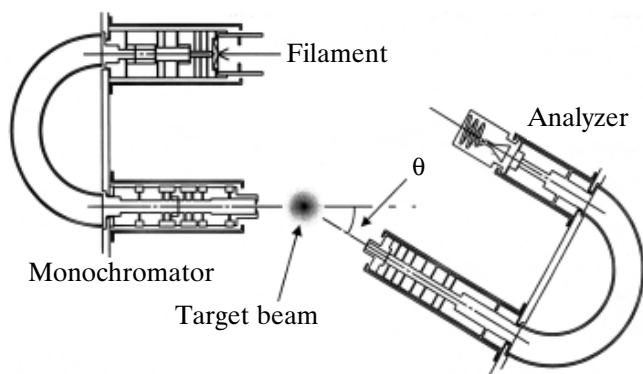


**Fig. 1.** Schematic diagram of the apparatus employed for the scattered electron measurements.

## Experimental

Electron impact excitation and dissociation have been performed using two experimental systems, both classed as Electron Scattering Spectrometers. One arrangement is used to detect scattered electrons, while the other is sensitive to negative and neutral fragments. The former spectrometer consists of an electron gun, an electron energy monochromator and analyzer, both hemispherical, and a channeltron detector, as shown in Fig. 1 [5]. The target gas is fed through an effusive nozzle to intersect the incident electron beam at right angles. The gun-monochromator and analyzer-detector systems are enclosed in differentially pumped boxes to reduce the effect of contaminating gases and to minimize the stray electron background. The scattered electrons are detected in the angular region between  $15^\circ$  and  $130^\circ$  with an angular resolution of  $\pm 1.5^\circ$ . The spectrometer has an overall energy resolution of 15–30 meV at impact energies from 1.5 to 100 eV. The incident electron energy is calibrated against the 19.3 eV resonance peak of He. The absolute normalization of the measured intensities has been performed by the relative flow method. Experimental errors are estimated to be 15–20% for and 20–30% for the elastic and inelastic scattering cross sections, respectively.

The second apparatus (Fig. 2) for electron-impact dissociation uses a cylindrical electrostatic energy selector to produce a beam of electrons at an incident angle variable from 0 to  $120^\circ$  with respect to a quadrupole mass spectro-

meter. This electron beam interacts with a gas beam produced at a nozzle. The stable negatively charged ion fragments formed at the intersection are detected at a selected angle by the QMS via a series of electron lenses. Neutral fragments produced by electron impact (i.e.  $\text{CH}_4 + e \rightarrow \text{CH}_3 + \text{H} + e$ ) effuse into a cell where they are ionized by a second electron beam ( $\text{CH}_3 + e \rightarrow \text{CH}_3^+ + 2e$ ) and channeled to the QMS for detection. For this electron collision, the appearance mass technique (also called the threshold ionization technique) is used to discriminate the fragments. The principle of the technique is based on the difference in ionization threshold (ion appearance potential) for the parent molecule (impact energy 14.3 eV,  $\text{CH}_4 + e \rightarrow \text{CH}_3^+ + \text{H} + 2e$ ) and for the dissociated fragments (impact energy 9.8 eV,  $\text{CH}_3 + e \rightarrow \text{CH}_3^+ + 2e$ ).

## Recent results and discussion

In this section text, we present selected results from the differential scattering experiments for the process  $e\text{-CF}_3\text{X}$  ( $\text{X} = \text{H}, \text{F}, \text{Cl}, \text{Br}, \text{I}$ ) that can be regarded as characteristic examples. Some preliminary results are also included on the formation of negative and neutral fragments from  $\text{SiF}_4$  and  $\text{CH}_4$  by electron impact.

### Elastic scattering: energy- and angular dependence

Figure 3 shows the elastic DCSs of  $\text{CF}_3\text{X}$  ( $\text{X} = \text{H}, \text{F}, \text{Cl}, \text{Br}, \text{I}$ ). At 1.5 eV, we observe a typical characteristic due to a long-range dipole interaction of polar molecules for  $\text{CF}_3\text{H}$  (1.65D) and  $\text{CF}_3\text{I}$  (0.92D), an intermediate trend for  $\text{CF}_3\text{Cl}$  (0.5D) and  $\text{CF}_3\text{Br}$  (0.65D), and a nonpolar feature for  $\text{CF}_4$ . From 8 to 10 eV, the DCSs can be seen to divide the species into two groups, one for  $\text{CF}_3\text{H}$  and  $\text{CF}_4$  [7] and the other for  $\text{CF}_3\text{Cl}$ ,  $\text{CF}_3\text{Br}$ , and  $\text{CF}_3\text{I}$ . For much higher energies, the DCSs show a similar angular dependence for all the molecules studied. Results in this energy region show the cross sections to be vibrationally elastic, i.e., a sum of over initial rotational states and an average over final rotational states. These DCSs can be used as the normalization standard for inelastic scattering cross sections as well as benchmark data required to guide development of theoretical models and computational schemes for calculating cross sections.

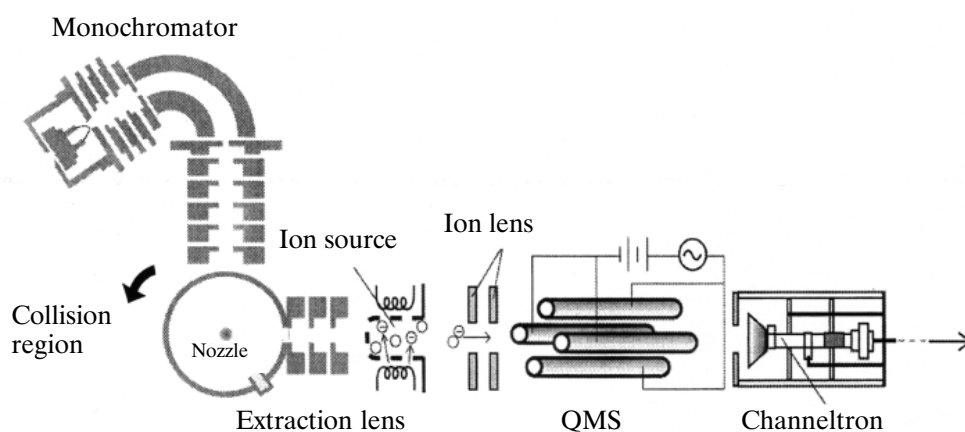


**Fig. 2.** Schematic diagram of the apparatus employed for the electron impact dissociation measurements.

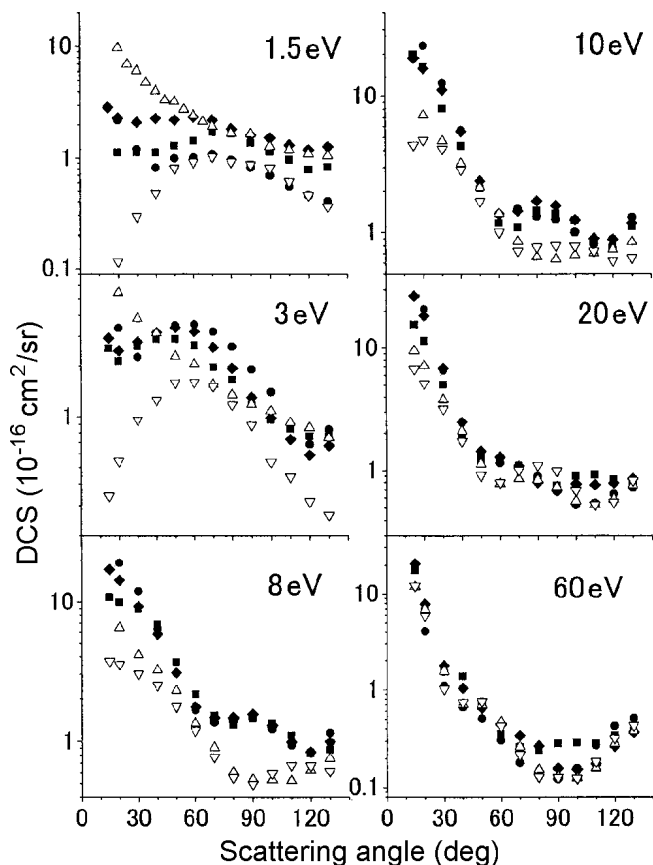


Fig. 3. Elastic DCS's of  $\text{CF}_3\text{X}$  ( $\text{X} = \text{H}(\Delta)$ ,  $\text{F}(\nabla)$ ,  $\text{Cl}(\blacksquare)$ ,  $\text{Br}(\blacklozenge)$ ,  $\text{I}(\bullet)$ ).

#### Vibrational excitation and resonance

$\text{CF}_3\text{X}$  molecules possess 6 fundamental vibrational modes. In general, resonances are difficult to observe by studying elastic interactions as strong direct scattering dominates, while the enhancement due to resonance appears clearly in vibrational excitations because the DCS for direct scattering is small. Figure 4 shows the vibrational excitation spectra of the unresolved composite modes (mainly  $\text{CF}_3$  stretching) of the 0.14 eV energy-loss peak for impact

energies from 1.5 to 14 eV, together with our previous results of  $\text{CF}_3\text{H}$  and  $\text{CF}_4$  ( $90^\circ$ ). A broad structure in the energy range of 7–9 eV, at a scattering angle of  $60^\circ$ , is clearly visible. The enhancement observed is attributed to a shape resonance associated with the formation of a short-lived negative ion. The DCSs presented are normalized to those of He by means of the relative-flow method. Each spectrum shows a steep increase in cross section, commonly starting around 3 eV, and a broad peak without fine structure in the energy region from 4 to 11 eV. These characteristics give sufficient evidence for short-lived shape resonance. The overall resonant features in  $\text{CF}_3\text{Cl}$  and  $\text{CF}_3\text{Br}$  are very similar to those found previously in studies of  $\text{CF}_3\text{I}$ . However, some different features may be noted. Firstly, the resonant DCS for  $\text{CF}_4$  shows a symmetric bell-shape with a peak at 8 eV, slightly higher than the peak positions observed for  $\text{CF}_3\text{X}$  ( $\text{X} = \text{H}, \text{Cl}, \text{Br}, \text{I}$ ). Secondly, the DCSs for  $\text{CF}_3\text{X}$  ( $\text{X} = \text{H}, \text{Cl}, \text{Br}, \text{I}$ ) have strongly asymmetric profiles. In particular, we observe a rapid rise in DCS at lower energies followed by a long tail with a weak shoulder at higher energies. The positions of these features are shifted gradually from 7 to 5.5 eV. Thirdly, the general shapes of the elastic DCSs for  $\text{CF}_3\text{H}$  and  $\text{CF}_4$  are close to each other around these resonant energies, while those of  $\text{CF}_3\text{Cl}$ ,  $\text{CF}_3\text{Br}$  and  $\text{CF}_3\text{I}$  are found to look quite similar to each other at all angles.

#### Low-lying electronic excitation and dissociation

These molecules are of further interest since analysis of their interactions can enable us to follow the changes that occur in the electronic structure and transitions of methane and the halogen lone pairs as a function of substitution and to gain knowledge on their excited states and ions. The electron energy loss spectra for the electronic states of  $\text{CF}_3\text{X}$  are presented in Fig. 5. Results are shown for impact energy 100 eV at scattering angle  $3^\circ$  or  $4^\circ$  and for 30 eV at  $15^\circ$ . In each of the  $\text{CF}_3\text{X}$  ( $\text{X} = \text{Cl}, \text{Br}, \text{I}$ ) plots, a broad and weak feature is observed, which is due to a transition promoting the X lone pair to a valence-shell orbital, anti-bonding in the C-X bond. No such transitions are found in the cases of  $\text{CF}_3\text{H}$  and  $\text{CF}_4$ . It should be noted that a similar low-lying electronic transition for  $\text{CF}_3\text{Cl}$  has been reported

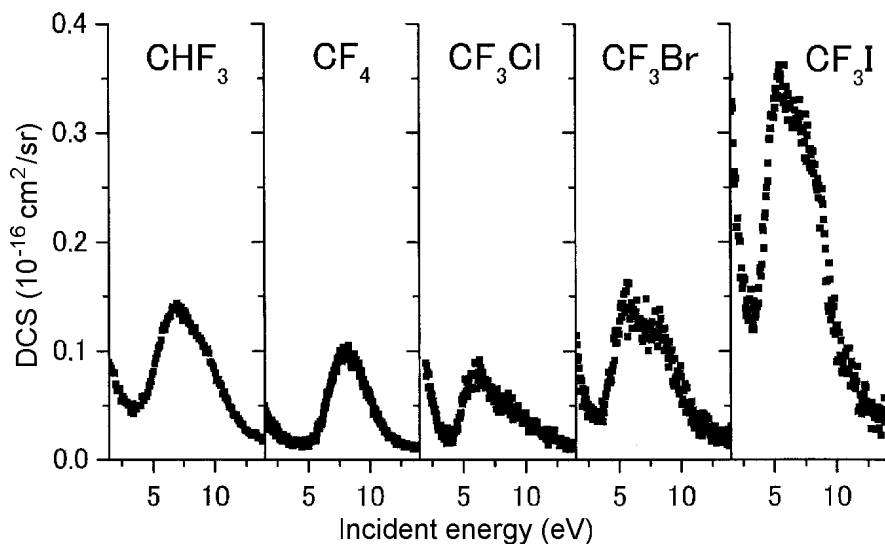
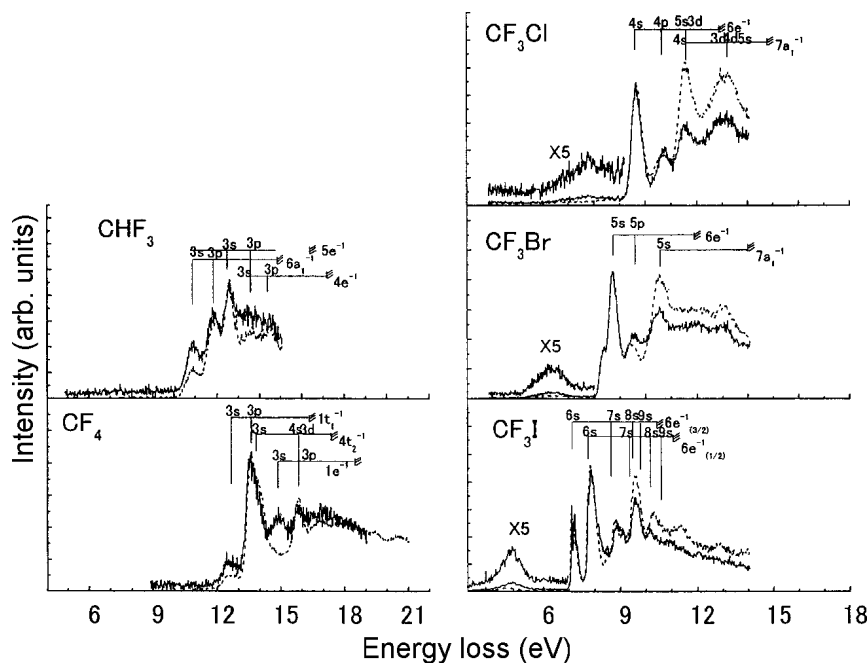
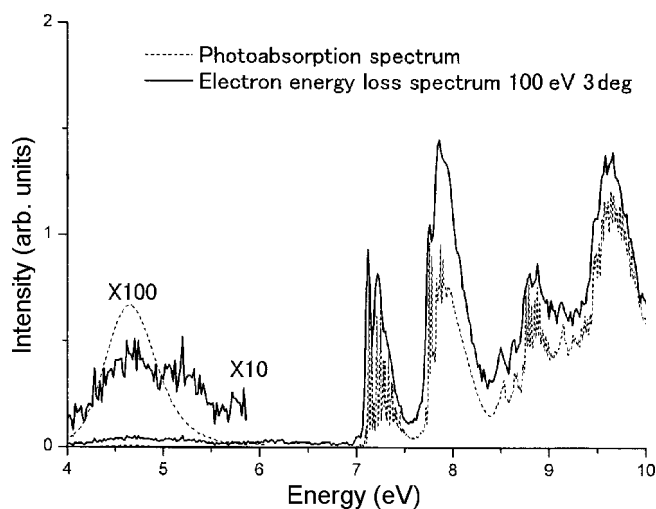


Fig. 4. Vibrational excitation DCS's of  $\text{CF}_3\text{X}$  ( $\text{X} = \text{H}, \text{F}, \text{Cl}, \text{Br}, \text{I}$ ).



**Fig. 5.** Electron energy loss spectra for electronic excitation of  $\text{CF}_3\text{X}$  ( $\text{X} = \text{H}, \text{F}, \text{Cl}, \text{Br}, \text{I}$ ). Solid curve; obtained at 30 eV 15 deg, and dotted curve; obtained at 100 eV, 4 deg, except for  $\text{CF}_3\text{H}$  and  $\text{CF}_3\text{I}$  obtained at 100 eV 3 deg.

in the momentum-transfer-resolved electron energy loss spectrum at impact energy 2.5 keV [8]. However, King and McConkey's measurement was not extended to sufficiently low energy to observe this feature in the high-resolution near-zero-angle EELS work [3]. Moreover, from *ab initio* GOS and single-excitation configuration calculations, we conclude that the transition corresponds to the  ${}^1\text{E} \leftarrow {}^1\text{A}_1(\text{LUMO} \leftarrow \text{HOMO})$  transition attributed partly to dipole allowed and, more strongly, to quadruple allowed interactions. Figure 6 shows the potential curves of the  ${}^1\text{E}$  and  $\text{A}_1$  along C-X (Cl, Br, I) bond direction, generating using the Gaussian basis sets. These results further suggest that the low-lying transition may correspond to excitation from a non-bonding state to a repulsive electronic state, subsequently causing the C-X bond to break apart. The spectra of  $\text{CF}_3\text{I}$  taken using high-energy electrons and low scattering angles also demonstrate excitation of the optically allowed states. This becomes clear when we compare the plots shown in Fig. 6 to the photoabsorption spectra [4].



**Fig. 6.** Electron energy loss spectrum and photoabsorption spectrum for  $\text{CF}_3\text{I}$ .

#### Electron-impact dissociation of molecules into negative and neutral fragments

Figure 7 shows the energy profiles of the fragment negative ions  $\text{F}^-$  and  $\text{SiF}_3^-$  observed from electron impact with  $\text{SiF}_4$ . In agreement with a previous study by Iga *et al.* [2], the pronounced peaks around 11 eV are attributed to dissociative electron attachment. Both fragments show a narrow resonance, with full width at half maximum of about 1 eV. The cross section for  $\text{F}^-$  formation shows a continuous increase from around 13 eV. As mentioned by Iga *et al.* [2], a possible mechanism for the formation of  $\text{F}^-$  at resonance is  $\text{SiF}_4 + e \rightarrow \text{SiF}_4^{*-} \rightarrow \text{F}^- + \text{SiF}_2 + \text{F}$ . Based on thermochemical values, it is estimated that the channel for  $\text{SiF}_4^-$  formation through the reaction  $\text{SiF}_4 + e \rightarrow \text{SiF}_4^{*-} \rightarrow \text{SiF}_3^- + \text{F}$  has a minimum energy requirement of 3.9 eV. However, the corresponding peak appears around 11 eV in Fig. 7. The excess energy can manifest itself as initial kinetic energy or electronic excitation of the dissociated fragments.

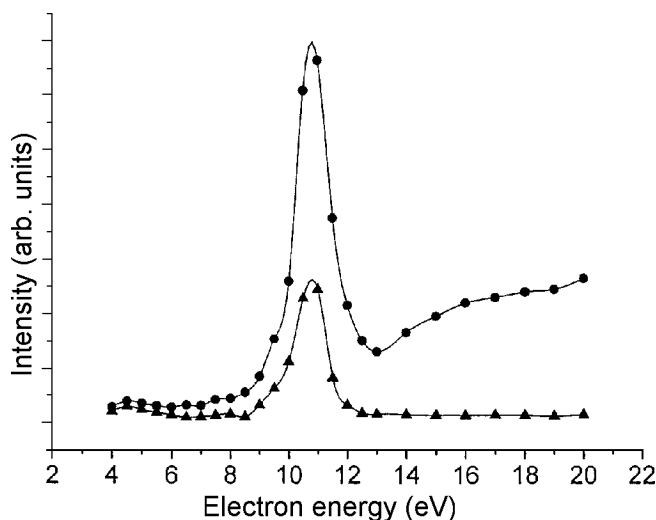


**Fig. 7.** Energy profiles of fragment negative ions of  $\text{F}^-$  ( $\bullet$ ) and  $\text{SiF}_3^-$  ( $\blacktriangle$ ).

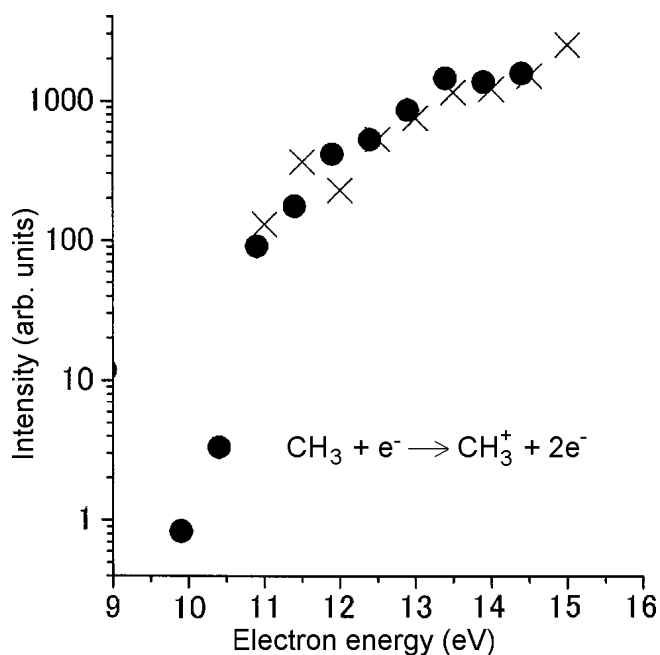


**Fig. 8.** Excitation function of  $\text{CH}_3^+$  from  $\text{CH}_3$  neutral fragment produced from  $\text{CH}_4$  by electron impact. •; present work, ×; H. Toyoda *et al.* [6].

Figure 8 shows the results of ionization threshold measurements of the  $\text{CH}_3$  neutral fragment from  $\text{CH}_4$  by electron impact. In this measurement, the impact energy of the monochromator is set at 11 eV (scattering angle  $45^\circ$ ), below the first ionization energy of the parent molecule, 14.3 eV. The neutral fragments produced are discriminated by means of the appearance mass technique, which is based on the difference in ionization threshold energy between the parent molecule (14.3 eV,  $\text{CH}_4 + e \rightarrow \text{CH}_3^+ + \text{H} + 2e$ ) and the produced fragments (9.8 eV,  $\text{CH}_3 + e \rightarrow \text{CH}_3^+ + 2e$ ). The signal must be treated further to remove background noise caused by fragments of  $\text{CH}_3$  dissociated thermally by the hot electron gun filaments and their surroundings surfaces. This discrimination can be achieved by pulsing the current on the filaments. As shown in Fig. 8, the threshold energy observed around 9.8 eV agrees very well with the data determined by flash photolysis optical absorption spectroscopy [1]. Above 11 eV, the present result reproduces the qualitative features of the ionization cross section of  $\text{CH}_3$  reported by Toyoda *et al.* [6].

## Conclusions

Selected results are summarized from the systematic measurement of absolute differential cross sections (DCSs) for electron scattering by halogen-containing molecules

$\text{CF}_3\text{X}$  (X = H, F, Cl, Br, I). A clear difference is demonstrated in the elastic-scattering cross section angular distributions of polar and nonpolar molecules with the substitution of one of the F atoms in  $\text{CF}_4$  for a H, Cl, Br or I atom. Vibrational excitation spectra of the unresolved composite modes (mainly  $\text{CF}_3$  stretching) for  $\text{CF}_3\text{X}$  reveal a common broad structure in the region from 7 to 9 eV due to shape resonance. Also observed is a low-lying electronic state of  $\text{CF}_3\text{Cl}$ ,  $\text{CF}_3\text{Br}$ , and  $\text{CF}_3\text{I}$ . This feature is enhanced at lower incident energies and larger scattering angles. Description of the apparatus and discussion of the operational principals of the experimental systems are included for the study of the electron-impact dissociation of molecules into negative and neutral fragments. Some preliminary results are presented on the formation of negative and neutral fragments by electron impact with  $\text{SiF}_4$  and  $\text{CH}_4$ .

**Acknowledgments** We are indebted to Dr N. J. Mason with whom the joint experimental research program has been developed. International exchange visits of authors (H. Tanaka and H. Cho) have been supported in part by the CUP (Core University Program, CR-01-02) of the Japan Society for the Promotion of Science. L. Pichl acknowledges partial support by JSPS Grant-in-Aid 21602/13/01073.

## References

1. Herzberg G (1966) Molecular spectra and molecular structure III. Electronic spectra and electronic structure of polyatomic molecules. Van Nostrand Reinhold, New York
2. Iga I, Rao MVVS, Srivastava SK, Nogueira JC (1992) Formation of negative ions by electron impact on  $\text{SiF}_4$  and  $\text{CF}_4$ . *Z Phys D: At Mol Clusters* 24:111–115
3. King GC, McConkey JW (1978) Electron energy-loss spectroscopy in the chloro-fluoro-methanes. *J Phys B: At Mol Opt Phys* 11:1861–1877
4. Mason NJ, Limao Vieira P, Eden S *et al.* (2002) VUV and low energy electron impact study of electronic state spectroscopy of  $\text{CF}_3\text{I}$ . *Int J Mass Spectrom* 12261:1–14
5. Tanaka S, Sueoka O (2001) Mechanisms of electron transport in electrical discharges and electron collision cross sections. *Adv At Mol Opt Phys* 44:1–31
6. Toyoda H, Kojima H, Sugai H (1989) Mass spectroscopic investigation of the  $\text{CH}_3$  radicals in a methane discharge. *Appl Phys Lett* 54:1507–1509
7. Varella MT do N, Winstead C, McKoy V, Kitajima M, Tanaka H (2002) Low-energy electron scattering by  $\text{CH}_3\text{F}$ ,  $\text{CH}_2\text{F}_2$ ,  $\text{CHF}_3$  and  $\text{CF}_4$ . *Phys Rev A* 65:022702–1–17
8. Ying JF, Mathers CP, Leung KT, Pritchard HP, Winstead C, McKoy V (1993) Observation of a “new” quadrupole transition at 7.7 eV in  $\text{CF}_3\text{Cl}$  by momentum-transfer-resolved electron energy loss spectroscopy. *Chem Phys Lett* 212:289–297